

## DATA REPOSITORY ITEM 2007186

### APPENDIX 1. FIELD RELATIONS

Figure A1.1 a) digital photograph of dacite dike field relations. Field of view ~1m b) annotated field sketch depicting structural sequence of granitic dike, pegmatite and quartz vein emplacement into Tethyan Sedimentary series metasediments (TSS) contemporaneous with top-to-south shear, followed by top-to-north shear band development in TSS (too small to be picked out clearly here). The ~ 20 cm thick dacite dike exhibits chilled margins, crosscuts all fabrics and is internally undeformed.

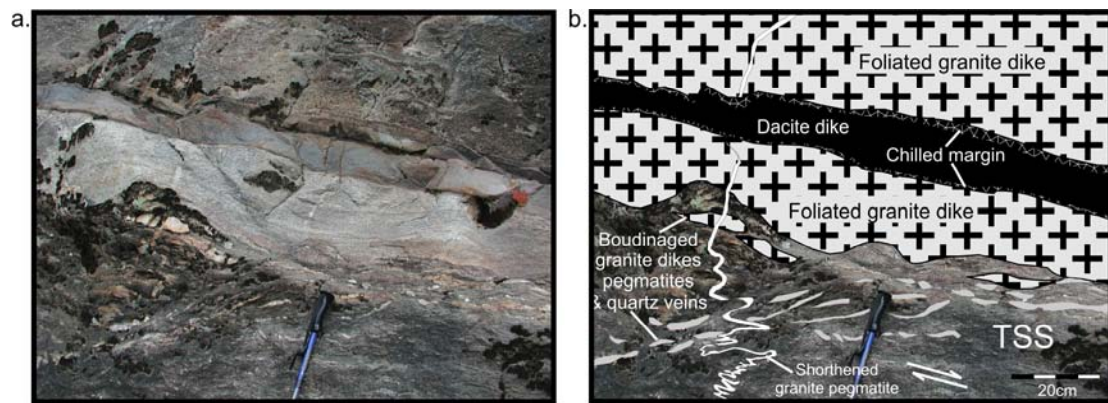


Figure A1.2 Sharp vertical contact of dacite dike with TSS. Strike of dike is approximately north, viewed towards west on the west side of Kuday valley ~ 1.5km north of Kuday village.



Figure A1.3 Dacite dike swarms (pale pink/buff linear features angling right) intruding TSS (dark grey to purple) north of Kuday village (bottom right foreground). View looking towards NNE.



Figure A1.4 Dacite dike swarms (pale pink/buff linear features angling right) intruding TSS (dark grey to purple) ~ 5km further north of Kuday (A1.3 image above). Strike of dikes N to NNW. View looking towards E



## APPENDIX 2. ANALYTICAL TECHNIQUES

Trace-element and Sr-Nd isotope analysis was undertaken to shed light on the provenance of the melts. We used LA-PIMMS and TIMS U-Pb dating of zircon and laser spot Ar-Ar analysis of biotite to ascertain intrusion ages of the dikes. Whole rock major and trace elements were analysed on an ARL Fisons wavelength-dispersive XRF spectrometer at the Open University. Major elements were determined using glass discs prepared by fusing powdered samples with Spectroflux 105. Rb, Sr, Ba, Zr, Y and Nb were determined from pressed powder pellets. Additional trace elements (REE, Ta, Th and U) were analysed by ICP-MS. 100 mg aliquots of powdered samples and standards were dissolved in PFA pressure vessels using 3ml TD HF and 1ml TD HNO<sub>3</sub> for a total of 48hrs on a hotplate at temperature 130°C, during which time solutions were sonicated once for a period of 20mins. Upon cooling, solutions were checked for clarity and evaporated to incipient dryness before being redissolved in 2ml concentrated TD HNO<sub>3</sub> and 4ml MilliQ deionised water at 130°C for 24hrs (plus a 20min sonication). This step was repeated with a further 24hr 3ml concentrated TD HNO<sub>3</sub> - 4ml MilliQ deionised water dissolution. After further evaporation to incipient dryness, samples were dissolved in 1 ml TD HNO<sub>3</sub> and diluted to 100ml using 18MΩ deionised water, and stored in clean polypropylene bottles. The solutions were analysed using an Agilent 7500s ICP-MS instrument, fitted with a Babington nebuliser operating at a flow rate of 0.4 ml min<sup>-1</sup>. Internal standards (Be, Rh, In, Tm, Re and Bi) were added on-line using a second peristaltic pump and residual drift for individual elements was assessed and corrected using repeat analyses of selected sample solutions. Standards used for calibration were BHVO-1, AC2/10, AGV-1, DNC-1, W-2, G-2 and RGM-1 and within run precision



was determined using repeat analyses of AC2/10 and G-2. In general, within-run precision is better than 2% r.s.d. for all elements and often better than 1%.

Nd and Sr isotope ratios were collected on a ThermoFinnigan Triton thermal ionization mass spectrometer (TIMS) at the Department of Earth Sciences, Open University. Standard sample preparation and isotopic analytical techniques are described in Cohen et al. (1988) and Charlier et al. (2006). Strontium was loaded in phosphoric acid on single Ta filaments, and the measured  $^{87}\text{Sr}/^{86}\text{Sr}$  ratios were corrected for instrumental mass fractionation using a  $^{87}\text{Sr}/^{88}\text{Sr} = 0.1194$  and the exponential fractionation law. Repeat analyses of the NBS987 Sr standard gave  $^{87}\text{Sr}/^{86}\text{Sr}$  ratios of  $0.710243 \pm 0.000014$  ( $2\sigma$ ) over the analysis period. Total procedural Sr blank was 20pg.  $^{87}\text{Rb}/^{86}\text{Sr}$  ratios were calculated from elemental ratios obtained by XRF.

Neodymium was loaded on double Re filaments and run as metal ions.  $^{143}\text{Nd}/^{144}\text{Nd}$  ratios were normalised to  $^{146}\text{Nd}/^{144}\text{Nd} = 0.7219$ . Repeat analyses of the Johnson-Matthey internal standard gave  $0.511817 \pm 0.000006$  ( $2\sigma$ ) for the period of sample analysis, corresponding to a value of BHVO-2 (external standard) of  $0.512976 \pm 14$  and LaJolla of  $0.511845 \pm 5$ . Total procedural Nd blanks were  $<1$  ng.  $^{147}\text{Sm}/^{144}\text{Nd}$  ratios were calculated from elemental ratios obtained from ICP-MS.

For Ar-isotope analysis, single biotite mineral grains were analysed using the Infrared laserprobe single-grain fusion technique. 30 biotite grains of grain size ca. 0.5 to 1mm were separated from each sample by standard mechanical crushing and sieving techniques followed by final hand-picking using tweezers and a binocular microscope to ensure purity. Altered or discoloured grains were discounted. Each biotite separate was cleaned ultrasonically in alternate ethanol and de-ionised water, prior to packaging in aluminium foil. Each individual foil packet contained a biotite

separate, and was bracketed by GA1550 biotite standards to monitor neutron flux during irradiation.

The samples were irradiated in two separate batches for 25 hours at the McMaster Reactor (Canada) in position 5C with cadmium shielding. Neutron flux was monitored using biotite mineral standard GA1550 which has an age of  $98.8 \pm 0.5$  Ma (Renne et al. 1998). The resulting J value =  $0.00592 \pm 0.00003$  (samples T108; T109) and J =  $0.00639 \pm 0.000032$  (samples T03/16a; JK3/17). Results were corrected for  $^{37}\text{Ar}$  decay, and neutron-induced interference reactions. The following correction factors were used:  $(^{39}\text{Ar}/^{37}\text{Ar})\text{Ca} = 0.00065$ ,  $(^{36}\text{Ar}/^{37}\text{Ar})\text{Ca} = 0.000264$ , and  $(^{40}\text{Ar}/^{39}\text{Ar})\text{K} = 0.0085$ ; based on analyses of Ca and K salts.

The irradiated samples were loaded into an ultra-high vacuum system and mounted on a New Wave Research UP-213 stage. A 1064nm CW Nd-YAG Spectron Ltd laser was focused into the sample chamber and was used to fuse individual biotite grains such that each grain yielded a single age. After each analysis the extracted gases were cleaned for 5 minutes using two SAES AP-10 getters running at  $450^\circ\text{C}$  and room temperature prior to automated inlet into an MAP 215-50 noble gas mass spectrometer. System blanks were measured before and after every two sample analyses and the mass discrimination value for atmospheric  $^{40}\text{Ar}/^{36}\text{Ar}$  was measured at 283. Isotopes of  $^{40}\text{Ar}$ ,  $^{39}\text{Ar}$ ,  $^{38}\text{Ar}$ ,  $^{37}\text{Ar}$ , and  $^{36}\text{Ar}$  were measured fifteen times per scan, and for ten scans, the final measurements are extrapolations back to the inlet time. All ages are reported at the  $2\sigma$  level and include a 0.5% error on the J value, weighted mean ages are calculated using Isoplot 3a (Ludwig, 2003).

U-Th-Pb isotopic measurements were made on zircon separated from the rock samples using standard techniques at the NERC Isotope Geosciences Laboratory, British Geological Survey, Keyworth. Minerals were analysed by ID-TIMS methods

on a single grain using a  $^{205}\text{Pb}$ - $^{233}\text{U}$ - $^{235}\text{U}$ - $^{230}\text{Th}$  tracer. For U and Pb, a Triton mass spectrometer was employed using single Re filaments and arrays of both faraday and ion counting detectors. Th isotopic measurements were made using a ThermoElemental Axiom ICPMC-MS using static measurement, with analysis of an in-house  $^{230}\text{Th}$ - $^{232}\text{Th}$  isotopic standard calibrated by the method outlined in Bowen et al. (1998) for measurement of mass bias. Chemical and mass spectrometric methods were as described in Parrish et al. (1987) and Noble et al. (1993). U and Pb blanks analysed averaged  $<0.4\text{pg}$  and  $<5\text{pg}$ , respectively. Decay constants used for  $^{238}\text{U}$ ,  $^{235}\text{U}$  and  $^{232}\text{Th}$  are those recommended by Steiger and Jäger (1977).

### APPENDIX 3. ZIRCON DESCRIPTION AND INTERPRETATION

Three zircon fractions were analysed from sample T108:

Z-1 A single very elongate euhedral grain with linear inclusions running the length of the crystal, which preclude the possibility of any older core, but contribute common Pb and therefore decreases the precision of the age.

Z-2 Three very clear euhedral grains (aspect ratio 3:1) with neither visible cores nor inclusions. The analysis shows inheritance and therefore indicates a core is present. An upper intercept on Concordia through 11.5 Ma yields a possible core age of  $987 \pm 57$  Ma, but given multiple grains, this yields a range, not a unique age of inherited zircon.

Z-3 Three euhedral grains (aspect ratio 3:1) with abundant inclusions; inheritance is clearly identified, with an upper intercept of  $1576 \pm 14$  Ma, but again this does not necessarily indicate a unique age of inheritance.

The Z-1 analysis is concordant yielding an age of  $11.49 \pm 0.14$  Ma. Th-Pb dating yields a  $^{208}\text{Pb}/^{232}\text{Th}$  age of  $12.22 \pm 0.84$ , within the quoted uncertainty of the U-Pb

age, but less precise due to the low Th content and relatively large common Pb correction.

The age of the dike is regarded therefore as  $11.5 \pm 0.1$  Ma. The age of inheritance is varied but lies within the range 980-1580 Ma.

## References

- Bowen, I., Walder, A.J., Hodgson, T., and Parrish, R.R., 1998, High precision and high accuracy isotopic measurement of uranium using lead and thorium calibration solutions by inductively coupled plasma multiple collector mass spectrometry, in Morrow, R.W., and Jeffrey, S.C., eds., Applications of Inductively Coupled Plasma Mass Spectrometry to Radionuclide Determinations: Second Volume, ASTM Special Technical Publication 1344., p. 21-26.
- Charlier, B.L.A., Ginibre, C., Morgan, D., Nowell, G.M., Pearson, D.G., Davidson, J.P., and Ottley, C.J., 2006, Methods for the microsampling and high-precision analysis of strontium and rubidium isotopes at single crystal scale for petrological and geochronological applications: Chemical Geology, v. (in press).
- Cohen, A.S., O'Nions, R.K., Siegenthaler, R., and Griffin, W.L., 1988, Chronology of the pressure-temperature history recorded by a granulite terrain: Contributions to Mineralogy and Petrology, v. 98, p. 303-311.
- DePaulo, D.J., 1981, Neodymium isotopes in the Colorado Front Range and implications for crust formation and mantle evolution in the Proterozoic: Nature, v. 291, p. 193-197.

- Ludwig, K.R., 2003, Users manual for Isoplot/Ex version 3.0: a geochronological toolkit for Microsoft Excel.: Berkeley Geochronology Center Spec. Pub. No. 4, 70 pp. Berkeley, California.
- Noble, S.R., Tucker, T.C., and Pharaoh, T.C., 1993, Lower Palaeozoic and Precambrian igneous rocks from eastern England, and their bearing on late Ordovician closure of the Tornquist Sea: constraints from U-Pb and Nd isotopes: *Geological Magazine.*, v. 130, p. 835-846.
- Parrish, R.R., Roddick, J.C., Loveridge, W.D., and Sullivan, R.W., 1987, Uranium-lead analytical techniques at the geochronology laboratory: Geological Survey of Canada, v. Special Paper 87-2, p. 3-7.
- Potts, P.J., Tindle, A.G., and Webb, P.C., 1992, Geochemical Reference Material Compositions: Whittles Publishing, Caithness, UK, 313 p.
- Renne, P.R., Swishe, C.C., Deino, A.L., Karner, D.B., Owens, T.L., and DePaulo, D.J., 1998, Intercalibration of standards, absolute ages and uncertainties in  $^{40}\text{Ar}/^{39}\text{Ar}$  dating: *Chemical Geology*, v. 145, p. 117-152.
- Steiger, R.H., and Jäger, E., 1977, Subcommittee on Geochronology: Convention on the use of decay constants in geo- and cosmochemistry: *Earth and Planetary Science Letters*, v. 36.



TABLE DR1. MAJOR, TRACE AND Sr, Nd ISOTOPIC DATA FOR SOUTHERN DIKE SWARM AND NYAINQENTANGLHA GNEISS

Sample	Kuday (dikes)									Nyainqentanglha	
	JK3/15	JK3/17	TO3/14i	SD52	SD51	JK3/16	T108	SD50	T109	G40	G38E
Rock type	Latite	Latite	Dacite	Dacite	Dacite	Dacite	Dacite	Rhyolite	Rhyolite	Gneiss	Gneiss
SiO <sub>2</sub>	61.01	61.21	63.68	63.71	65.10	67.11	67.56	71.29	72.62	71.88	72.31
TiO <sub>2</sub>	0.83	0.84	0.81	0.63	0.66	0.48	0.62	0.22	0.21	0.29	0.39
Al <sub>2</sub> O <sub>3</sub>	18.10	18.27	17.96	16.16	17.45	16.96	17.29	15.96	16.04	14.26	13.45
Fe <sub>2</sub> O <sub>3</sub> †	4.70	4.76	3.16	2.40	2.99	2.48	0.45	1.37	0.04	2.13	2.17
MnO	0.07	0.07	0.04	0.04	0.05	0.04	0.05	0.02	0.02	0.03	0.04
MgO	1.7	1.7	1.1	0.9	1.0	0.9	1.0	0.5	0.6	0.4	0.6
CaO	4.84	4.58	2.57	4.01	4.28	2.54	3.96	1.71	1.73	1.36	1.64
Na <sub>2</sub> O	4.01	4.22	4.36	4.67	4.66	4.59	4.07	5.21	4.76	3.15	2.96
K <sub>2</sub> O	3.02	1.96	4.02	1.82	1.61	3.11	0.95	2.67	2.12	5.60	5.44
P <sub>2</sub> O <sub>5</sub>	0.33	0.32	0.22	0.23	0.24	0.17	0.24	0.11	0.02	0.08	0.13
LOI	1.10	1.03	1.36	4.73	1.22	1.53	1.11	0.71	0.86	0.31	0.30
Total	99.73	98.98	99.29	99.26	99.23	99.94	99.60	99.74	99.79	99.44	99.48
Rb	84	74	133	56	75	97	59	93	40	299	237
Sr	1595	1572	1269	769	1672	885	1458	676	366	210	360
Ba	1184	1230	1434	984	1662	703	1494	479	476	562	507
Y	13	12	10	6	9	7	9	7	6	14	11
Zr	158	154	204	131	156	137	125	100	90	220	190
Nb	7	8	9	4	6	4	5	2	3	9	29
Th	15.1	15.9	33.5	27.1	24.2	5.9	20.2	4.2	3.2	74.2	87.6
U	4.9	2.6	5.7	6.2	6.2	4.3	5.2	3.9	2.4	9.2	8.0
Ta	0.51	0.51	0.55		0.39	0.37	0.38	0.25	0.27	1.73	3.41
La	49.60	49.77	74.05		56.15	22.78	43.87	15.00	10.67	67.94	90.10
Ce	97.99	97.15	138.12		106.63	46.37	90.59	29.50	23.01	168.67	184.70
Pr	12.15	12.02	15.61		12.64	5.54	9.31	3.70	2.54	18.23	20.05
Nd	45.51	44.33	52.58		44.77	20.55	35.72	13.98	10.12	58.36	63.12
Sm	7.78	7.61	7.78		7.11	3.82	5.70	2.89	2.18	8.23	8.77
Eu	1.79	1.73	1.69		1.52	0.85	1.18	0.70	0.53	0.88	1.29
Gd	4.80	4.65	4.43		3.93	2.59	3.44	2.11	1.77	4.80	5.10
Tb	0.56	0.55	0.51		0.42	0.33	0.36	0.26	0.25	0.56	0.65
Dy	2.58	2.51	2.27		1.84	1.54	1.62	1.15	1.24	2.86	2.99
Ho	0.45	0.43	0.40		0.30	0.26	0.28	0.19	0.22	0.62	0.54
Er	1.12	1.04	0.99		0.73	0.64	0.70	0.46	0.53	1.86	1.39
Yb	0.82	0.74	0.73		0.51	0.47	0.60	0.32	0.42	1.30	1.10
Lu	0.11	0.09	0.09		0.06	0.06	0.09	0.04	0.06	0.15	0.14
<sup>87</sup> Rb/ <sup>86</sup> Sr	0.15	0.13	0.30		0.13	0.31	0.12	0.39	0.31	4.07	1.71

DR2007186

3ES

TABLE DR2. Ar-Ar DATA FOR BIOTITE GRAINS FROM SOUTHERN DIKES

Sample	$^{40}\text{Ar}/^{39}\text{Ar}$	$^{38}\text{Ar}/^{39}\text{Ar}$	$^{37}\text{Ar}/^{39}\text{Ar}$	$^{36}\text{Ar}/^{39}\text{Ar}$	$^{39}\text{Ar}^*$	$^{40}\text{Ar}^*/^{39}\text{Ar}$	Age (Ma)	$\pm$
T109								
Biotite 1	1.636	0.0067	-0.0020	0.0010	30.61	1.353	14.39	
Biotite 2	1.729	0.0128	0.0001	0.0017	94.34	1.229	13.08	
Biotite 3	1.744	0.0110	0.0003	0.0025	80.18	1.001	10.66	
Biotite 4	1.610	0.0128	-0.0002	0.0019	90.72	1.063	11.31	
Biotite 5	1.713	0.0087	0.0004	0.0026	79.23	0.946	10.07	
Biotite 6	1.589	0.0103	0.0003	0.0019	129.83	1.035	11.02	
Biotite 7	1.735	0.0115	0.0011	0.0023	110.53	1.051	11.19	
Biotite 8	1.755	0.0105	0.0005	0.0023	114.43	1.061	11.30	
Biotite 9	1.815	0.0132	0.0020	0.0027	66.42	1.011	10.77	
Biotite 10	1.671	0.0095	0.0024	0.0025	43.47	0.928	9.89	
Calculated age							11.21	
* Amounts of $^{39}\text{Ar}$ are $\times 10^{-12}$ cc STP								
J value = 0.00592 $\pm$ 0.00003								
JK3/16a								
Biotite 1	3.486	0.0147	0.0024	0.0092		0.772	8.41	
Biotite 2	2.809	0.0138	0.0042	0.0065		0.886	9.64	
Biotite 3	3.348	0.0141	0.0023	0.0086		0.793	8.63	
Biotite 4	3.017	0.0142	0.0016	0.0072		0.876	9.54	
Biotite 5	3.190	0.0139	0.0020	0.0079		0.846	9.21	
Biotite 6	3.387	0.0149	0.0023	0.0089		0.756	8.23	
Calculated age							9.13	
* Amounts of $^{39}\text{Ar}$ are $\times 10^{-12}$ cc STP								
J value = 0.00604 $\pm$ 0.00003								

TABLE DR3. U-Pb-Th ISOTOPIC DATA FOR ANALYSED ZIRCON GRAINS FROM DIKE (T108)

Analysis*	Weight	U	Th	Pb**	<sup>206</sup> Pb^	<sup>208</sup> Pb^	Pb^^	Th***	<sup>206</sup> Pb^A	1 std err	<sup>207</sup> Pb^A	1 std err	<sup>207</sup> Pb^A	1 std err	<sup>208</sup> Pb^A	1 std err	<sup>206</sup> Pb^A	2 std err	<sup>207</sup> Pb^A	2 std err	<sup>208</sup> Pb^A	2 std err
	(mg)	(ppm)	(ppm)	(ppm)	<sup>204</sup> Pb	<sup>204</sup> Pb	(pg)	U	<sup>238</sup> U	(%)	<sup>235</sup> U	(%)	<sup>206</sup> Pb	(%)	<sup>232</sup> Th	(%)	<sup>238</sup> U	(Ma)	<sup>235</sup> U	(Ma)	<sup>232</sup> Th	(Ma)
Z-1, (1), 5:1, ε	0.0033	1404	634	2.61	83	54.92	8.0	0.49	0.001791	0.67	0.01179	3.20	0.0478	2.8	0.0006047	4.8	11.54	0.15	11.90	0.8	12.22	0
Z-2, (3), 3:1, ε	0.0032	601	nd	6.59	181	77.21	7.1	0.75	0.009741	0.39	0.09106	1.39	0.0678	1.2	nd	nd	62.49	0.48	88.49	2.4	nd	
Z-3, (3), 3:1, ε	0.0048	3567	nd	16.90	1429	125.61	3.6	0.19	0.004828	0.18	0.05273	0.23	0.0792	0.12	nd	nd	31.05	0.11	52.17	0.2	nd	

\* Z= zircon, (2)= number of crystals in analysis, 5:1=aspect rati, eu=euhedral, incl=abundant inclusions

\*\* radiogenic Pb

\*\*\* atomic ratio of Th to U, calculated from radiogenic <sup>208</sup>Pb/<sup>206</sup>Pb

^ Measured ratio, corrected for spike and Pb fractionation (0.09%/amu)

^^ Total common Pb in analysis, corrected for fractionation and spike

^A Corrected for blank Pb and U, and common Pb (Stacey-Kramers model Pb equivalent to interpreted age of mineral)

nd, not determined; Th isotopes were only measured for concordant analysis Z-1